Population transfer via a decaying state

N. V. Vitanov* and S. Stenholm
Helsinki Institute of Physics, P.O. Box 9, Siltavuorenpenger 20C, FIN-00014 University of Helsinki, Helsinki, Finland
(Received 31 March 1997)

The paper examines the effect of irreversible dissipation from the intermediate state on the efficiency of population transfer by partially overlapping delayed pulses in three-state systems. Several general approximations to the final-state population for both the intuitive and counterintuitive pulse sequences are derived. They show that the loss of transfer efficiency is much stronger for the intuitive pulse sequence, as then the intermediate state is significantly populated during the transfer. For the counterintuitive sequence, the damping of the final-state population is found to be exponential for small decay rates and polynomial for large ones; moreover, the range of decay rates, over which the transfer efficiency remains high, is proportional to the squared pulse area. The paper also presents an analytically solvable model, involving smooth delayed pulses, as well as numerical results and analytic approximations for Gaussian pulses. [S1050-2947(97)03708-6]

PACS number(s): 32.80.Bx, 33.80.Be, 42.50.−p

I. INTRODUCTION

The stimulated Raman adiabatic passage (STIRAP) is a well established technique for selective and efficient population transfer to a particular excited atomic or molecular state ([1–3] and references therein). STIRAP transfers adiabatically population between two states $|1\rangle$ and $|3\rangle$ via an intermediate state $|2\rangle$ by means of two partially overlapping delayed laser pulses in a counterintuitive order. The initial state $|1\rangle$ and the final state $|3\rangle$ have to be on two-photon resonance, while the intermediate state $|2\rangle$ can be off resonance by a certain detuning Δ. The population is transferred via an eigenstate $|0\rangle$ of the Hamiltonian, which is a linear superposition of the bare states $|1\rangle$ and $|3\rangle$ only. In *the adiabatic limit*, no population resides in state $|2\rangle$ at any time and hence, its properties do not influence the transfer efficiency. Beyond the adiabatic limit (i.e., for finite pulse areas), the transfer efficiency is generally less than unity and the intermediate state *is* populated during the excitation (as well as after it). We have recently shown [3] that for fixed pulse areas, the transfer efficiency is adversely affected by the detuning Δ as it deteriorates the adiabaticity of the process. Moreover, the detuning range over which the transfer efficiency remains high ($\geqslant \frac{1}{2}$) has been found to be proportional to the squared pulse area.

Another factor, which is expected to deteriorate the population transfer, is the dissipation from the intermediate state $|2\rangle$. In this paper, we examine the dependence of the STIRAP efficiency on the rate Γ of irreversible decay of this state out of the three-state system. Besides being interesting by itself, this problem is also closely related to population transfer via a continuum [4–6] and to the problem of transitions in a dissipative two-state system [7,8]. The paper is organized as follows. In Sec. II, we provide the basic equations and definitions as well as some general approximations and conclusions about the effect of the intermediate-state decay. In Sec. III, we present an analytically solvable model involving smooth delayed pulses, which illustrates our general conclusions. In Sec. IV, we analyze, numerically and analytically, population transfer with Gaussian pulses. Finally, in Sec. V, we summarize the main results.

II. DEFINITION OF THE PROBLEM AND GENERAL PROPERTIES

A. The three-state system

The three-state Λ system under consideration is shown schematically in Fig. 1. States $|1\rangle$ and $|2\rangle$ are coupled by the pump-laser pulse $\Omega_p(t)$, while states $|2\rangle$ and $|3\rangle$ are coupled by the Stokes-laser pulse $\Omega_s(t)$. The direct transition between states $|1\rangle$ and $|3\rangle$ is electric-dipole forbidden. Two-photon resonance between states $|1\rangle$ and $|3\rangle$ is maintained. The intermediate state $|2\rangle$ is off-resonance by a detuning Δ and decays out of the system by a certain mechanism (e.g., spontaneous emission, collisional relaxation, or ionization) with a total decay rate $\Gamma \geqslant 0$. The pulse durations are supposed to be short compared with the relaxation times within the system, so that spontaneous emission from state $|2\rangle$ to states $|1\rangle$ and $|3\rangle$ is neglected. The probability amplitudes of the three states satisfy the Schrödinger equation which in the rotating-wave approximation has the form

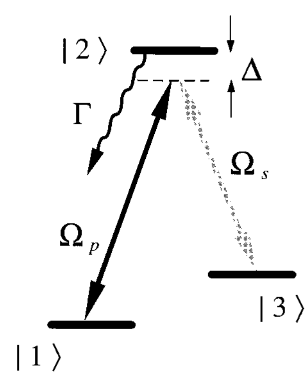

FIG. 1. The three-state Λ system. The initial state $|1\rangle$ and the final state $|3\rangle$ are on two-photon resonance. The intermediate state $|2\rangle$ is off single-photon resonance by a detuning Δ and decays out of the system with a rate Γ. In STIRAP the Stokes pulse Ω_s precedes the pump pulse Ω_p (counterintuitive pulse order).

*Electronic address: vitanov@rock.helsinki.fi

$$i\frac{d}{dt}\begin{bmatrix} c_1 \\ c_2 \\ c_3 \end{bmatrix} = \begin{bmatrix} 0 & \Omega_p & 0 \\ \Omega_p & \Delta - i\Gamma & \Omega_s \\ 0 & \Omega_s & 0 \end{bmatrix} \begin{bmatrix} c_1 \\ c_2 \\ c_3 \end{bmatrix}. \tag{1}$$

The functions $\Omega_p(t)$ and $\Omega_s(t)$, representing the Rabi frequencies of the two pulses, and the (constant) detuning Δ will be assumed positive as the populations do not depend on their signs. Furthermore, $\Omega_p(t)$ and $\Omega_s(t)$ are supposed to be pulse-shaped functions that vanish at infinity and whose pulse areas are finite, $\int_{-\infty}^{\infty}\Omega_{p,s}(t)\ dt<\infty$. We assume that at the initial time $t\to-\infty$ the three-state system is in its ground state $|1\rangle$,

$$c_1(-\infty)=1, \quad c_2(-\infty)=0, \quad c_3(-\infty)=0,$$

and we are interested in the populations at $t\to+\infty$, $P_n=|c_n(+\infty)|^2$ $(n=1,2,3)$. Finally, we will suppose for simplicity that the two pulses have the same peak strength α/T and characteristic width T,

$$\Omega_p(t)=\frac{\alpha}{T}f_p(t/T), \quad \Omega_s(t)=\frac{\alpha}{T}f_s(t/T),$$

where α is a dimensionless positive parameter proportional to the pulse area, while the functions $f_p(t/T)$ and $f_s(t/T)$ describe the pulse shapes. It is also useful to introduce the dimensionless detuning δ and decay rate γ,

$$\delta=\Delta T, \quad \gamma=\Gamma T.$$

B. Adiabatic representation

1. Adiabatic states

The adiabatic states are defined as the instantaneous eigenstates of the Hamiltonian in Eqs. (1). In the absence of decay $(\Gamma=0)$, they are given by [2,3]

$$|+\rangle=\sin\varphi\ \sin\vartheta|1\rangle+\cos\varphi|2\rangle+\sin\varphi\ \cos\vartheta|3\rangle, \tag{2a}$$

$$|0\rangle=\cos\vartheta|1\rangle-\sin\vartheta|3\rangle, \tag{2b}$$

$$|-\rangle=\cos\varphi\ \sin\vartheta|1\rangle-\sin\varphi|2\rangle+\cos\varphi\ \cos\vartheta|3\rangle, \tag{2c}$$

where Euler's angles $\vartheta(t)$ and $\varphi(t)$ are defined as

$$\tan\vartheta(t)=\frac{\Omega_p(t)}{\Omega_s(t)}, \quad \tan 2\varphi(t)=\frac{2\Omega_0(t)}{\Delta(t)}, \tag{3}$$

and $\Omega_0(t)=\sqrt{\Omega_p^2(t)+\Omega_s^2(t)}$. The probability amplitudes $a_+(t)$, $a_0(t)$, and $a_-(t)$ of the adiabatic states are connected to the bare (diabatic) amplitudes by the orthogonal rotation

$$\begin{bmatrix} c_1 \\ c_2 \\ c_3 \end{bmatrix} = \begin{bmatrix} \sin\varphi\ \sin\vartheta & \cos\vartheta & \cos\varphi\ \sin\vartheta \\ \cos\varphi & 0 & -\sin\varphi \\ \sin\varphi\ \cos\vartheta & -\sin\vartheta & \cos\varphi\ \cos\vartheta \end{bmatrix} \begin{bmatrix} a_+ \\ a_0 \\ a_- \end{bmatrix}.$$

In the adiabatic representation, Eqs. (1) become

$$i\frac{d}{dt}\begin{bmatrix} a_+ \\ a_0 \\ a_- \end{bmatrix} = \begin{bmatrix} \Omega_0\cot\varphi - i\Gamma\cos^2\varphi & i\dot\vartheta\sin\varphi & i\dot\varphi+\frac{1}{2}i\Gamma\sin 2\varphi \\ -i\dot\vartheta\sin\varphi & 0 & -i\dot\vartheta\cos\varphi \\ -i\dot\varphi+\frac{1}{2}i\Gamma\sin 2\varphi & i\dot\vartheta\cos\varphi & -\Omega_0\tan\varphi - i\Gamma\sin^2\varphi \end{bmatrix} \begin{bmatrix} a_+ \\ a_0 \\ a_- \end{bmatrix}, \tag{4}$$

where an overdot denotes a time derivative. The adiabatic behavior is reached in the limit of large pulse amplitudes and/or large pulse widths, i.e., for large pulse areas.

2. Population transfer in the absence of dissipation

In STIRAP the pulses are applied in the *counterintuitive* order, that is the Stokes pulse Ω_s precedes the pump pulse Ω_p. Hence, $\lim_{t\to-\infty}[\Omega_p(t)/\Omega_s(t)]=0$, $\lim_{t\to+\infty}[\Omega_p(t)/\Omega_s(t)]=\infty$, which implies that $\vartheta^{ci}(-\infty)=0$, $\vartheta^{ci}(+\infty)=\pi/2$. Hereafter the superscript "ci" ("i") denotes the counterintuitive (intuitive) pulse sequence. If the excitation is adiabatic then the population is transferred from state $|1\rangle$ to state $|3\rangle$ via the adiabatic state $|0\rangle$ which is equal to state $|1\rangle$ at $t\to-\infty$ and to state $|3\rangle$ at $t\to+\infty$.

In the *intuitive* pulse order, the pump pulse Ω_p comes first, which means that $\vartheta^i(-\infty)=\pi/2$, $\vartheta^i(+\infty)=0$. For $\Delta=0$, the adiabatic states are given by superpositions of bare states at both $t\to-\infty$ and $t\to+\infty$; this gives rise to oscillations in the populations. For $\Delta\neq 0$, the population is transferred from state $|1\rangle$ to state $|3\rangle$ via the adiabatic state $|-\rangle$, which is equal to state $|1\rangle$ at $t\to-\infty$ and to state $|3\rangle$ at $t\to+\infty$. Thus, in the absence of dissipation, both pulse orders produce complete population transfer for $\Delta\neq 0$ in the adiabatic limit [2].

It is intuitively clear that the intermediate-state decay must reduce the transfer efficiency and that this effect is much stronger for the intuitive order. This is so because in the adiabatic regime no population visits the intermediate state at any time for the counterintuitive order, while this state *is* populated during the transfer for the intuitive order [9]. From the adiabatic point of view [Eqs. (4)], the difference between the two orders arises from the fact that the adiabatic state $|0\rangle$ does not decay, while $|-\rangle$ does with a rate $\Gamma\sin^2\varphi$.

From now on we will assume that we are in the *near-adiabatic regime*, where the transfer efficiency is almost unity in the absence of dissipation $(\gamma=0)$ (for the intuitive order we also suppose that $\delta\neq 0$). To ensure a large transfer for $\gamma=0$, we have to assume that $\alpha^2\gg\delta,1$ [3]. Given this, we wish to find *how* the transfer efficiency decreases with γ [10] and for any fixed set of pulse parameters, we wish to determine the value $\gamma_{1/2}$ at which $P_3=\frac{1}{2}$.

C. Population transfer by the intuitive pulse sequence in the presence of dissipation

The adiabatic state $|-\rangle$, which transfers the population from state $|1\rangle$ to state $|3\rangle$ for $\Delta\neq 0$ for the intuitive sequence, decays with a rate $\Gamma\,\sin^2\varphi$. As follows from Eqs. (4), in the adiabatic limit the final population of state $|3\rangle$ for intuitive pulses is

$$P_3^i \approx \exp\left[-2\Gamma\int_{-\infty}^{\infty}\sin^2\varphi(t)\,dt\right] = \exp\left\{-\Gamma\int_{-\infty}^{\infty}\left[1-\frac{\Delta}{\sqrt{\Delta^2+4\Omega_0^2(t)}}\right]dt\right\}. \tag{5}$$

Certainly, losses in P_3^i may also occur due to nonadiabatic transitions from state $|-\rangle$ to states $|0\rangle$ and $|+\rangle$, but the main loss mechanism in the near-adiabatic regime is the direct dissipation from $|-\rangle$. Thus we expect an *exponential* decay of P_3^i against Γ. Moreover, P_3^i *increases* with Δ [unless Δ is too large and deteriorates the adiabaticity; then Eq. (5) is invalid], which has to be expected as Δ suppresses the intermediate-state population. Finally, P_3^i *decreases* with α, which means that improving adiabaticity reduces, rather than enhances, the transfer.

D. Population transfer by the counterintuitive pulse sequence in the presence of dissipation

1. Loss mechanisms

It is less obvious how the transfer efficiency decreases with Γ for the counterintuitive order. Then the losses in the transfer efficiency occur in two ways. First, inasmuch as the excitation is never perfectly adiabatic, during the transfer some population visits the intermediate state where it is exposed to *dissipation*. In the adiabatic picture, this loss mechanism corresponds to nonadiabatic transitions from state $|0\rangle$ to states $|-\rangle$ and $|+\rangle$ with subsequent dissipation from these latter states. The difference between the cases of $\Gamma=0$ and $\Gamma\neq 0$ arises from the fact that for $\Gamma=0$, some of the population transferred to states $|-\rangle$ and $|+\rangle$ returns to state $|0\rangle$ by the end of the excitation. This derives from higher-order adiabatic processes and can be understood by means of the superadiabatic approach of Berry [11]. For $\Gamma\neq 0$, the population in states $|-\rangle$ and $|+\rangle$ is exposed to irreversible dissipation and the probability for such a return is much smaller [12].

The second, more subtle, mechanism of transfer efficiency loss is the *quantum overdamping*. It is similar to that in two-state systems [8] and shows up as effective decoupling of the three states at large Γ. Consequently, at large Γ the population remains predominantly in the initial state, both the transfer to state $|3\rangle$ and the dissipation losses being suppressed.

Both mechanisms — dissipation and overdamping — lead to a loss of transfer efficiency. Thus, P_3^{ci} should decrease steadily with Γ. We expect the dissipation to dominate at small to moderate Γ, while we expect the overdamping to show up at large Γ. We will see that these two mechanisms lead to different dependences of P_3^{ci} on Γ. On the other hand, as a result of the overdamping, P_1^{ci} is expected to increase at large Γ and eventually to tend to unity at very large Γ. The population loss $P_{loss}^{ci}=1-P_1^{ci}-P_3^{ci}$ should increase initially, reach a maximum at some moderate Γ, and then decrease at large Γ. Below, we consider several general approximations to P_3^{ci} in the limiting cases of weak and strong dissipation.

2. Weak dissipation

When α is large compared with γ, the diagonal elements in the equations for a_+ and a_- in Eqs. (4) dominate over the nondiagonal ones. Then we can carry out adiabatic elimination of states $|+\rangle$ and $|-\rangle$ by setting $a_+=\dot{a}_-=0$ in Eqs. (4) and eliminating a_+ and a_- from the resulting set of two algebraic equations. Since $P_3^{ci}(\infty)=|a_0(\infty)|^2$, we obtain

$$P_3^{ci}\approx\exp\left[-2\Gamma\int_{-\infty}^{\infty}\frac{\dot{\vartheta}^2(t)}{\Omega_0^2(t)+\dot{\varphi}^2(t)}dt\right] \quad (\alpha\gg\sqrt{\gamma^2+\delta^2},1), \tag{6}$$

assuming that the integral converges. Similarly to Eq. (5) for the intuitive sequence, Eq. (6) shows an *exponential* dependence of P_3^{ci} on Γ, but the damping rate is considerably smaller. It also exhibits rather different dependences on α and δ. Namely, P_3^{ci} *increases* with α as the adiabaticity improves, while P_3^{ci} depends (via $\dot{\varphi}$) *very weakly* on δ (decreases), because in the denominator Ω_0^2 dominates over $\dot{\varphi}^2$ in the near-adiabatic regime.

3. Strong dissipation: effective two-state problem, dark and bright states

For large decay rates, we can eliminate adiabatically the intermediate state $|2\rangle$ by setting $dc_2/dt=0$ in Eqs. (1), determining c_2 from the resulting algebraic equation, and substituting it in the other two equations [2,3]. Adiabatic elimination of the intermediate states is a widely used approximation in N-state systems on $(N-1)$-photon resonance [13]. In this approximation, our three-state system on two-photon resonance is reduced to a two-state system consisting of states $|1\rangle$ and $|3\rangle$ and described by the equations

$$i\frac{d}{dt}\begin{bmatrix}c_1\\c_3\end{bmatrix}\approx-\frac{1}{\Delta-i\Gamma}\begin{bmatrix}\Omega_p^2 & \Omega_p\Omega_s\\ \Omega_p\Omega_s & \Omega_s^2\end{bmatrix}\begin{bmatrix}c_1\\c_3\end{bmatrix} \quad (\sqrt{\gamma^2+\delta^2}\gg\alpha,1). \tag{7}$$

Similar equations appear in the problem of population transfer via a continuum [4–6].

The time-dependent transformation

$$\begin{bmatrix}c_1\\c_3\end{bmatrix}=\begin{bmatrix}\cos\vartheta & \sin\vartheta\\ -\sin\vartheta & \cos\vartheta\end{bmatrix}\begin{bmatrix}a_d\\a_b\end{bmatrix}, \tag{8}$$

where $\vartheta(t)$ is given by Eq. (3), casts Eqs. (7) into their adiabatic representation

$$i\frac{d}{dt}\begin{bmatrix}a_d\\a_b\end{bmatrix}=\begin{bmatrix}0 & -i\dot{\vartheta}\\ i\dot{\vartheta} & \tilde{\Delta}-i\tilde{\Gamma}\end{bmatrix}\begin{bmatrix}a_d\\a_b\end{bmatrix}, \tag{9}$$

$$\tilde{\Gamma}(t)=\frac{\Gamma\Omega_0^2(t)}{\Gamma^2+\Delta^2},\quad \tilde{\Delta}(t)=-\frac{\Delta\Omega_0^2(t)}{\Gamma^2+\Delta^2}.$$

The amplitudes a_b and a_d correspond to states $|b\rangle=\sin\vartheta|1\rangle+\cos\vartheta|3\rangle$ and $|d\rangle=\cos\vartheta|1\rangle-\sin\vartheta|3\rangle$, referred to as the *bright and dark states*, respectively. Notice that the dark state coincides with the adiabatic state $|0\rangle$, Eq. (2b). Equations (9) show that in the adiabatic-elimination approximation the three-state system is equivalent to a system of two states $|b\rangle$ and $|d\rangle$, with coupling $i\dot{\vartheta}$, detuning $\tilde{\Delta}$ and decay rate $\tilde{\Gamma}$ of state $|b\rangle$. As follows from Eqs. (8), the counterintuitive pulse order corresponds to initial conditions $a_d(-\infty)=1$, $a_b(-\infty)=0$, and the population P_3^{ci} of state $|3\rangle$ is equal to the probability of remaining in the dark state $|d\rangle$. In contrast, the intuitive order requires initial conditions $a_b(-\infty)=1$, $a_d(-\infty)=0$, and P_3^i is equal to the probability of remaining in the (decaying) bright state $|b\rangle$.

For $\alpha^2\ll\sqrt{\gamma^2+\delta^2}$, the two-state problem (9) is nearly resonant. Since the area of the coupling $\dot{\vartheta}$ is $\pi/2$, the two-state system is almost inverted which implies that both P_3^{ci} and P_3^i vanish, as should be the case. For $\alpha^2\gg\sqrt{\gamma^2+\delta^2}$, the two states $|b\rangle$ and $|d\rangle$ are effectively decoupled and the transition between them is suppressed. Thus, as α increases, P_3^{ci} approaches unity while P_3^i vanishes. Hence, for the counterintuitive order, Eqs. (7) and (9) have the correct $\gamma=0$ limit and should provide a good approximation even for small γ, although formally they do not have to. For the intuitive order, Eqs. (7) do not give the correct limit for small γ and can only be used for large γ.

Equations (7) show that the populations depend on α, δ, and γ only through the ratio $\alpha^2/(\delta-i\gamma)$. For the counterintuitive order, this should be the case practically for any values of α, δ, and γ (given that α is large, which is assumed throughout the paper). This suggests that on resonance, the populations depend on the ratio α^2/γ only and hence, the width $\gamma_{1/2}$ of the range of high transfer efficiency for counterintuitive pulses must scale as α^2,

$$\gamma_{1/2}\approx c\alpha^2\quad(\delta=0),\tag{10}$$

where c is a coefficient that may depend on the specific pulse shapes and the pulse delay but not on γ and α. This quadratic dependence is similar to that of $\delta_{1/2}$ on α for $\gamma=0$ [3]. For $\delta\neq0$, a more complicated dependence is to be expected. However, we will see in Sec. IV that $\gamma_{1/2}$ depends only very slightly on δ.

4. Very strong dissipation: the Magnus approximation

For $\sqrt{\gamma^2+\delta^2}\gg\alpha^2$, P_3 can be estimated by means of the Magnus approximation [14], applied to Eqs. (7). It gives, for either pulse orders,

$$P_3\approx\frac{1}{2}\exp\left(-\frac{2\gamma S_p}{\gamma^2+\delta^2}\right)\left[\cosh\left(-\frac{2\gamma S}{\gamma^2+\delta^2}\right)\right.$$
$$\left.-\cos\left(-\frac{2\delta S}{\gamma^2+\delta^2}\right)\right],$$

where $S=\int_{-\infty}^{\infty}\Omega_p(t)\Omega_s(t)dt$, $S_{p,s}=\int_{-\infty}^{\infty}\Omega_{p,s}^2(t)dt$. For simplicity, we assume equal areas, $S_p=S_s$. As $S,S_{p,s}\propto\alpha^2\ll\sqrt{\gamma^2+\delta^2}$, this approximation has the asymptotic behavior

$$P_3\sim\frac{S^2}{\gamma^2+\delta^2},\quad(\alpha^2\ll\sqrt{\gamma^2+\delta^2}).\tag{11}$$

Hence, at very large γ, the transfer efficiency vanishes in a Lorentzian *power* law, rather than exponentially.

III. ANALYTIC MODEL

A. The model

The model is introduced by means of the functions

$$\Omega_1(t)=\Omega_0(t)\cos[\pi s(t)/2],\tag{12a}$$

$$\Omega_2(t)=\Omega_0(t)\sin[\pi s(t)/2],\tag{12b}$$

where

$$\Omega_0(t)=\frac{\alpha}{T}f\left(\frac{t}{T}\right),$$

$$s(t)=\frac{1}{T}\int_{-\infty}^{t}f^2\left(\frac{t'}{T}\right)dt'=\int_{-\infty}^{t/T}f^2(x)dx.\tag{13}$$

The parameter α is dimensionless and is proportional to the pulse area. It plays the role of the adiabaticity parameter, i.e., the larger α, the stronger the adiabaticity. The parameter T has the dimension of time and determines the time and frequency scales. Both α and T will be assumed positive without loss of generality. We also suppose that $f(x)$ is an *arbitrary* smooth pulse-shaped function which vanishes at infinity, $f(\pm\infty)=0$, and is normalized to unity, $\int_{-\infty}^{\infty}f^2(x)dx=1$. Then, as time runs from $-\infty$ to $+\infty$, $s(t)$ changes from 0 to 1. We emphasize that Eqs. (12) define a *class* of models rather than a single model; the members of this class can be obtained by choosing different functions $f(x)$ with the properties specified above. The final populations for all models of this class are the same and depend on α only; their time evolutions, however, depend on the specific model because $s(t)$ is different. As an example, let $f(x)=1/\sqrt{2}\ \operatorname{sech}x$; then

$$\Omega_1(t)=\frac{\alpha}{T\sqrt{2}}\operatorname{sech}\left(\frac{t}{T}\right)\cos\left[\frac{\pi}{4}\left(\tanh\frac{t}{T}+1\right)\right],\tag{14a}$$

$$\Omega_2(t)=\frac{\alpha}{T\sqrt{2}}\operatorname{sech}\left(\frac{t}{T}\right)\sin\left[\frac{\pi}{4}\left(\tanh\frac{t}{T}+1\right)\right].\tag{14b}$$

The pulse $\Omega_1(t)$ precedes the pulse $\Omega_2(t)$ and their maxima are separated by a fixed pulse delay of about 0.772 T. The pulse areas are both approximately equal to 1.338α. We point out that model (12) is not the same as the analytic models used in Refs. [2,3].

By applying either Ω_1 on the pump transition and Ω_2 on the Stokes transition or vice versa, we can realize both pulse orders. Namely, for $\Omega_p=\Omega_2$ and $\Omega_s=\Omega_1$ we have the counterintuitive order, while for $\Omega_p=\Omega_1$ and $\Omega_s=\Omega_2$ we have the intuitive order.

Model (12) allows exact analytic solution of Eqs. (7) [although this solution is approximate for Eqs. (1) since Eqs. (7) are an approximation to Eqs. (1)]. The derivation is straightforward and we do not present it explicitly here. It is obtained by changing the independent variable in Eqs. (7) from t to s. Then we go to the adiabatic representation (9) where the Hamiltonian becomes constant and the equations are easily solved.

B. On-resonance solution

On resonance ($\Delta=0$), the population evolutions of the dark and bright states for *counterintuitive* pulses ($\Omega_p=\Omega_2$, $\Omega_s=\Omega_1$) are given by

$$P_d^{ci}(t)=|a_d(t)|^2, \tag{15}$$

$$P_b^{ci}(t)=|a_b(t)|^2, \tag{16}$$

while those of states $|1\rangle$ and $|3\rangle$ read

$$P_1^{ci}(t)=[a_d(t)\cos\vartheta(t)+a_b(t)\sin\vartheta(t)]^2, \tag{17}$$

$$P_3^{ci}(t)=[-a_d(t)\sin\vartheta(t)+a_b(t)\cos\vartheta(t)]^2, \tag{18}$$

with

$$a_d(t)=e^{-\xi\vartheta(t)}\Bigg\{\cosh[\vartheta(t)\sqrt{\xi^2-1}] + \frac{\xi}{\sqrt{\xi^2-1}}\sinh[\vartheta(t)\sqrt{\xi^2-1}]\Bigg\},$$

$$a_b(t)=e^{-\xi\vartheta(t)}\frac{\sinh[\vartheta(t)\sqrt{\xi^2-1}]}{\sqrt{\xi^2-1}},$$

where $\vartheta(t)=\pi s(t)/2$, and $\xi=\alpha^2/\pi\gamma$. In the above equations, the relations $\sqrt{\xi^2-1}=i\sqrt{1-\xi^2}$, $\sinh(ix)=i\sin x$ and $\cosh(ix)=\cos x$ have to be used for $\xi<1$. The time evolutions of the populations for the specific pulses (14) are plotted in Fig. 2 for $\alpha=10$ and $\gamma=10$, along with the pulse shapes. A very good agreement between the exact numerical results and our analytic approximations (15)–(18) is observed.

The population of state $|3\rangle$ at $t\to\infty$ for *counterintuitive* pulses ($\Omega_p=\Omega_2$, $\Omega_s=\Omega_1$) is

$$P_3^{ci}=e^{-\pi\xi}\left[\cosh\left(\frac{1}{2}\pi\sqrt{\xi^2-1}\right) + \frac{\xi}{\sqrt{\xi^2-1}}\sinh\left(\frac{1}{2}\pi\sqrt{\xi^2-1}\right)\right]^2, \tag{19}$$

while for the *intuitive* pulse order ($\Omega_p=\Omega_1$, $\Omega_s=\Omega_2$) it is

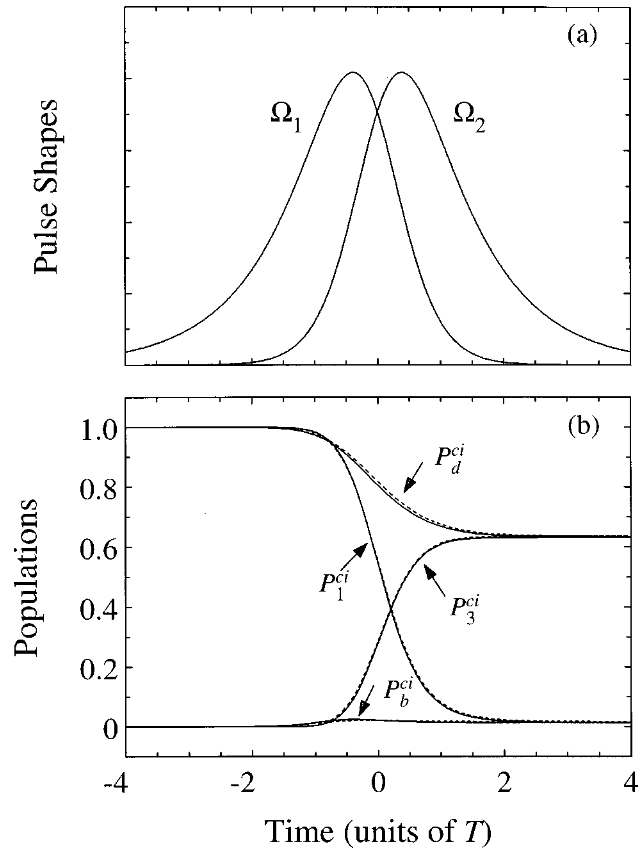

FIG. 2. (a) The pulse shapes (14). (b) The population evolutions of the dark and bright states $|d\rangle$ and $|b\rangle$ and those of states $|1\rangle$ and $|3\rangle$ for the pulses (14), applied in the counterintuitive order, with $\alpha=10$ and $\gamma=10$. The exact values, obtained by the numerical integration of Eqs. (1), are plotted by solid curves, while the dashed curves show the analytic formulas (15)–(18).

$$P_3^{i}=e^{-\pi\xi}\left[\cosh\left(\frac{1}{2}\pi\sqrt{\xi^2-1}\right) - \frac{\xi}{\sqrt{\xi^2-1}}\sinh\left(\frac{1}{2}\pi\sqrt{\xi^2-1}\right)\right]^2. \tag{20}$$

The population of state $|1\rangle$ is the same for both pulse orders,

$$P_1^{ci}=P_1^{i}=e^{-\pi\xi}\left[\frac{\sinh\left(\frac{1}{2}\pi\sqrt{\xi^2-1}\right)}{\sqrt{\xi^2-1}}\right]^2, \tag{21}$$

which is a consequence of the symmetry of the problem [2]. Equations (19)–(21) depend on α and γ only through the ratio $\xi=\alpha^2/\pi\gamma$, since they are derived from Eqs. (7).

In the limit $\xi\gg1$, i.e., for $\alpha^2\gg\pi\gamma$, we obtain from Eq. (19) that

$$P_3^{ci}\sim e^{-\pi/2\xi}=e^{-\pi^2\gamma/2\alpha^2}, \quad (\alpha^2\gg\pi\gamma). \tag{22}$$

This is exactly the result predicted by the approximation (6) for model (12), i.e., we find an exponential dependence of P_3^{ci} on γ for small γ.

For $\xi\ll1$, i.e., for $\alpha^2\ll\pi\gamma$, we have

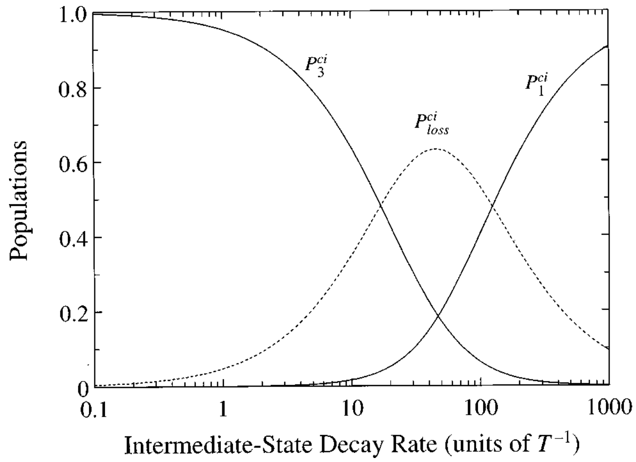

FIG. 3. The populations of the initial state P_1^{ci}, the final state P_3^{ci}, and the population loss P_{loss}^{ci} against the intermediate-state decay rate for the pulses (12), applied in the counterintuitive order, for $\alpha=10$ and $\delta=0$.

$$P_1^{ci}=P_1^i\sim 1-\pi\xi+O(\xi^2),$$

$$P_3^{ci}\sim\xi^2[1-\pi\xi/2+O(\xi^2)],$$

$$P_3^i\sim\xi^2[1-3\pi\xi/2+O(\xi^2)].$$

Thus, in the limit of large γ, we come across the effect of quantum overdamping as $P_1^{ci}=P_1^i\rightarrow 1$. We also see that then $P_3\sim(\alpha^2/\pi\gamma)^2$, in agreement with the Magnus approximation (11) [since $S=\alpha^2/\pi$ for model (12)].

In Fig. 3, we have plotted the populations (21) and (19) of states $|1\rangle$ and $|3\rangle$ and the population loss $P_{loss}^{ci}=1-P_1^{ci}-P_3^{ci}$ for the counterintuitive sequence against the decay rate γ for $\alpha=10$. Our analytic results almost coincide with the exact values (not shown). The ultimate decrease of the population loss at large γ is a result of quantum overdamping. The overall behavior of P_1^{ci}, P_3^{ci} and P_{loss}^{ci} is in complete agreement with the general conclusions of Sec. II D 1. Finally, Eq. (22) gives the value $(2/\pi^2)\ln 2\approx 0.1405$ for the coefficient c in Eq. (10), which reproduces fairly well the numerically obtained value 0.1591.

C. Nonzero detuning

For $\Delta\neq 0$, the final-state population for *counterintuitive* pulses ($\Omega_p=\Omega_2$, $\Omega_s=\Omega_1$) is

$$P_3^{ci}=\frac{e^{-\pi\xi}}{4(\mu^2+\nu^2)}\{e^{\pi\mu}[(\mu+\xi)^2+(\nu+\eta)^2]+e^{-\pi\mu}[(\mu-\xi)^2+(\nu-\eta)^2]+2(\mu^2+\nu^2-\xi^2-\eta^2)\cos\pi\nu-4(\mu\eta-\nu\xi)\sin\pi\nu\}, \tag{23}$$

where

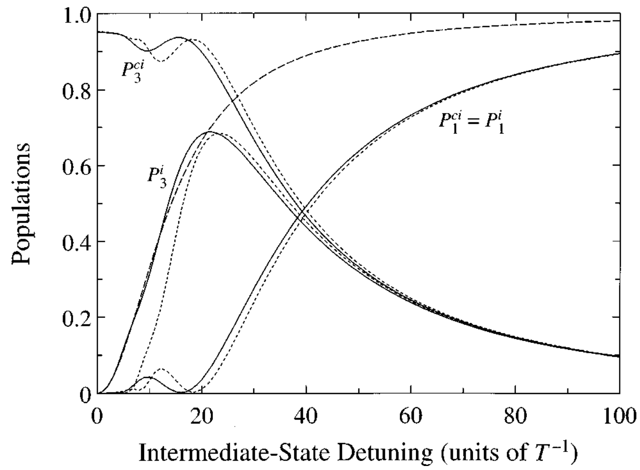

FIG. 4. The populations of the states $|1\rangle$ and $|3\rangle$ for the intuitive and counterintuitive pulse orders plotted against the intermediate-state detuning for model (12) with $\alpha=10$ and $\gamma=1$. The exact values, obtained by numerical integration of Eqs. (1), are plotted by solid curves, while the short-line dashed curves show the analytic formulas (23), (24), and (26). The long-line dashed curve is the approximation (25) for P_3^i.

$$\xi=\frac{\gamma\alpha^2}{\pi(\gamma^2+\delta^2)},\qquad \eta=\frac{\delta\alpha^2}{\pi(\gamma^2+\delta^2)},$$

$$\mu=\sqrt{\frac{1}{2}[\sqrt{(\xi^2-\eta^2-1)^2+4\xi^2\eta^2}+\xi^2-\eta^2-1]},$$

$$\nu=\sqrt{\frac{1}{2}[\sqrt{(\xi^2-\eta^2-1)^2+4\xi^2\eta^2}-(\xi^2-\eta^2-1)]}.$$

For the *intuitive* pulse order ($\Omega_p=\Omega_1$, $\Omega_s=\Omega_2$), the final-state population is given by

$$P_3^i=\frac{e^{-\pi\xi}}{4(\mu^2+\nu^2)}\{e^{\pi\mu}[(\mu-\xi)^2+(\nu-\eta)^2]+e^{-\pi\mu}[(\mu+\xi)^2+(\nu+\eta)^2]+2(\mu^2+\nu^2-\xi^2-\eta^2)\cos\pi\nu+4(\mu\eta-\nu\xi)\sin\pi\nu\}. \tag{24}$$

As we discussed in Sec. II D 3, Eqs. (7) do not produce the correct final-state population for the intuitive order for $\sqrt{\gamma^2+\delta^2}\ll\alpha^2$; thus, Eqs. (20) and (24) do not give the correct results either. The relevant approximation in this case is Eq. (5) which gives for model (14)

$$P_3^i\approx\left(1+\frac{2\alpha^2}{\delta^2}\right)^{-\gamma},\quad (\alpha^2\gg\sqrt{\gamma^2+\delta^2},1). \tag{25}$$

The initial-state population is the same for both pulse orders,

$$P_1^i=P_1^{ci}=\frac{e^{-\pi\xi}}{2(\mu^2+\nu^2)}(\cosh\pi\mu-\cos\pi\nu). \tag{26}$$

In Fig. 4, the populations (23)–(26) are plotted against the intermediate-state detuning δ for $\alpha=10$ and $\gamma=1$ and compared to the exact numerical values. As expected, the final-state population P_3^i for the intuitive order is approximated

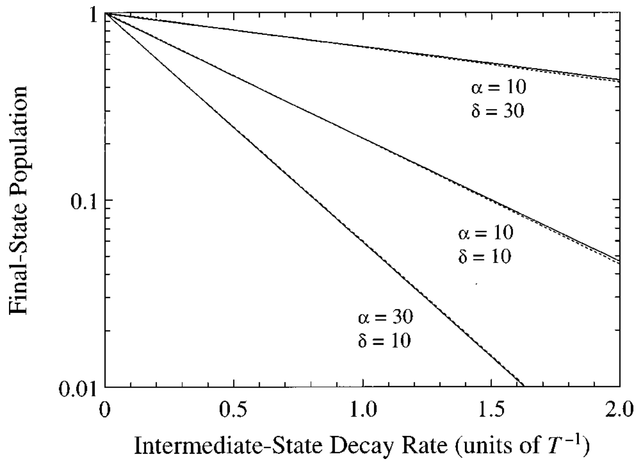

FIG. 5. The final-state population as a function of the intermediate-state decay rate for the Gaussian model (27) with $\tau=-0.5$ T (*intuitive* pulse order), for several values of α and δ (shown nearby each curve). The full curves show the exact results, obtained by numerical integration of Eqs. (1), while the dashed curves derive from our analytic approximation (5).

well by Eq. (25) for small δ and by Eq. (24) for large δ. It increases initially as δ reduces the intermediate-state population and hence, the population loss. At large δ, P_3 is nearly the same for both pulse orders and decreases with δ due to the deteriorating adiabaticity. This behavior is similar to that in the absence of dissipation [3].

IV. GAUSSIAN PULSES

The experimentally most interesting pulse shape is Gaussian. We consider two Gaussian pulses of the same widths and strengths but separated by a time delay of 2τ,

$$\Omega_p(t)=\frac{\alpha}{T}\exp\left[-\left(\frac{t-\tau}{T}\right)^2\right],\quad \Omega_s(t)=\frac{\alpha}{T}\exp\left[-\left(\frac{t+\tau}{T}\right)^2\right], \tag{27}$$

where α and T are positive parameters while τ can be positive (counterintuitive pulse order) or negative (intuitive order). The parameter α is dimensionless while T and τ have the dimension of time.

A. Intuitive pulse order

In Fig. 5, the final-state population P_3^i is plotted as a function of $\gamma\equiv\Gamma T$ for several combinations of α and $\delta\equiv\Delta T$, chosen to ensure near-adiabatic regime and almost complete transfer at $\gamma=0$. The time delay is $\tau=-0.5$ T. The simple analytic approximation (5) is seen to be very accurate and the exponential dependence on γ is clearly demonstrated. As Eq. (5) predicted, P_3^i decreases with the pulse area, while it increases with the detuning (unless the detuning is very large and violates the adiabaticity). We have also calculated the exact P_3^i for $\alpha=\delta=30$ (not shown) and we have found that it practically coincides with the curve for $\alpha=\delta=10$, in agreement with Eq. (5), which suggests that in the near-adiabatic regime P_3^i depend on α and δ only via the ratio α/δ.

B. Counterintuitive pulse order

The analytic approximation (6), shown to give the correct behavior for model (12) and a good approximation to the coefficient c in Eq. (10), does not apply to Gaussians because then, as one can easily check, the integral in Eq. (6) is divergent. It is possible to modify this approximation by taking finite integration limits. This requires careful determination of the time interval where the ''essential'' changes in the population dynamics take place. However, this approach is very sensitive to the choice of these limits and hence, ambiguous.

We have estimated P_3^{ci} analytically using another approach presented below. It is similar to that in Ref. [3] and is based on Eqs. (7). We cannot find analytically the exact solution of Eqs. (7) for model (27), but we can approximate it by using some of the known two-state solutions. The most relevant to our problem is the model

$$\widetilde{\Omega}_p(t)=\frac{1}{T}f\left(\frac{t}{T}\right)\sqrt{\sqrt{x^2(t)+1}+x(t)}, \tag{28a}$$

$$\widetilde{\Omega}_s(t)=\frac{1}{T}f\left(\frac{t}{T}\right)\sqrt{\sqrt{x^2(t)+1}-x(t)}, \tag{28b}$$

$$x(t)=\kappa\tan\frac{\pi z(t)}{2\zeta},\quad z(t)=\frac{1}{T}\int_0^t f^2\left(\frac{t'}{T}\right)dt',$$

where $f(t)$ is a symmetric pulse-shaped function and $\zeta\equiv z(\infty)$. As time runs from $-\infty$ to ∞, z changes from $-\zeta$ to ζ. By means of the transformation

$$c_{1,3}(t)=b_{1,3}(t)\exp\left\{\frac{i}{2(\Delta-i\Gamma)}\int_0^t[\widetilde{\Omega}_p^2(t')+\widetilde{\Omega}_s^2(t')]dt'\right\},$$

Eqs. (7) take the form

$$i\frac{d}{dt}\begin{bmatrix}b_1\\ b_3\end{bmatrix}\approx\begin{bmatrix}-\widetilde{\Delta}_{eff} & \widetilde{\Omega}_{eff}\\ \widetilde{\Omega}_{eff} & \widetilde{\Delta}_{eff}\end{bmatrix}\begin{bmatrix}b_1\\ b_3\end{bmatrix},$$

where

$$\widetilde{\Omega}_{eff}(t)=-\frac{\widetilde{\Omega}_p(t)\widetilde{\Omega}_s(t)}{\Delta-i\Gamma}=-\frac{f^2(t/T)}{T^2(\Delta-i\Gamma)}, \tag{29a}$$

$$\widetilde{\Delta}_{eff}(t)=\frac{\widetilde{\Omega}_p^2(t)-\widetilde{\Omega}_s^2(t)}{2(\Delta-i\Gamma)}=\frac{\kappa f^2(t/T)}{T^2(\Delta-i\Gamma)}\tan\frac{\pi z(t)}{2\zeta}. \tag{29b}$$

The same quantities for the Gaussian model (27) are

$$\Omega_{eff}(t)=-\frac{\alpha^2}{T^2(\Delta-i\Gamma)}e^{-2(t^2+\tau^2)/T^2}, \tag{30a}$$

$$\Delta_{eff}(t)=\frac{\alpha^2}{T^2(\Delta-i\Gamma)}e^{-2(t^2+\tau^2)/T^2}\sinh\frac{4\tau t}{T^2}. \tag{30b}$$

Model (29) is a generalization [for complex parameters and $f^2(t)\propto\mathrm{sech}(t/T_0)$] of the Allen-Eberly model [15], $\Omega_{AE}(t)$

$\propto \text{sech}(t/T_0)$, $\Delta_{AE}(t) \propto \tanh(t/T_0)$, which is a particular case of the Demkov-Kunike model [16] and can be solved analytically.

Model (28) resembles model (27) in the sense that $\tilde{\Omega}_p(t)$ and $\tilde{\Omega}_s(t)$ are pulse shaped, have equal areas, and $\tilde{\Omega}_s(t)$ precedes $\tilde{\Omega}_p(t)$. Their shapes, however, are not Gaussian. In order to compensate this difference as much as possible, we have determined the free parameters in such a way that the maxima (at $t=0$) and the pulse areas of $\Omega_{eff}(t)$ and $\tilde{\Omega}_{eff}(t)$ as well as the slopes of $\Delta_{eff}(t)$ and $\tilde{\Delta}_{eff}(t)$ at the crossing ($t=0$) are the same. This leads to

$$\zeta = \alpha^2 \sqrt{\pi/8} e^{-2(\tau/T)^2}, \quad \kappa = \frac{\tau}{T}\sqrt{8/\pi}, \quad f^2(0) = \alpha^2 e^{-2(\tau/T)^2}.$$

Equations (7) with model (28) can be solved in a similar fashion as in Refs. [16,17]; the solution is

$$P_3^{ci} \approx \left| \frac{\Gamma^2\left(B+\frac{1}{2}\right)}{\Gamma(B+\sqrt{B^2-A^2})\Gamma(B-\sqrt{B^2-A^2})} \times e^{-2B\ \ln(2B/A)+2\sqrt{B^2-A^2}\ln[B/A+\sqrt{(B/A)^2-1}]} \right|^2, \quad (31)$$

where

$$A = \frac{2\zeta}{\pi} = \frac{1}{\sqrt{2\pi}} \frac{\alpha^2 e^{-2(\tau/T)^2}}{\gamma + i\delta}, \quad B = A\kappa = \frac{2}{\pi}\frac{\tau}{T}\frac{\alpha^2 e^{-2(\tau/T)^2}}{\gamma + i\delta}.$$

This solution is exact for model (28) but it is approximate for the Gaussian pulses (27). Equation (31) is plotted in Fig. 6, along with the exact numerical solution for the Gaussian pulses (27), for several values of the pulse delay τ in the case when $\alpha=20$ and $\delta=0$. The analytic approximation (31) is very accurate throughout except for some discrepancy for $\tau=0.25$ T. Note the huge difference in the decay rate scales in Fig. 5, where the pulse order is intuitive, and Fig. 6.

We now turn to the derivation of the value $\gamma_{1/2}$, at which $P_3^{ci}=\frac{1}{2}$. We have obtained it numerically by solving Eqs. (1) for various fixed α. Then, by plotting $\gamma_{1/2}$ against α we have checked that the dependence (10) holds very well at large α, from where we have determined the coefficient c. This coefficient depends on the pulse delay, which can also be concluded from Fig. 6, where the rate of damping of P_3^{ci} with γ is seen to depend on τ. On the other hand, the dependence of c on τ/T can be determined approximately from Eq. (31) when for any fixed τ/T, we solve the equation $P_3^{ci}=\frac{1}{2}$ for A. It is possible to obtain a simple approximate expression. By applying the Stirling's asymptotic expansion [18]

$$\ln\Gamma(z) \sim \tfrac{1}{2}\ln(2\pi) + (z-\tfrac{1}{2})\ln z - z + \frac{1}{12z} + O(|z|^{-3}), \quad (|\arg z|<\pi, |z|\gg 1)$$

to the gamma functions in Eq. (31), we obtain

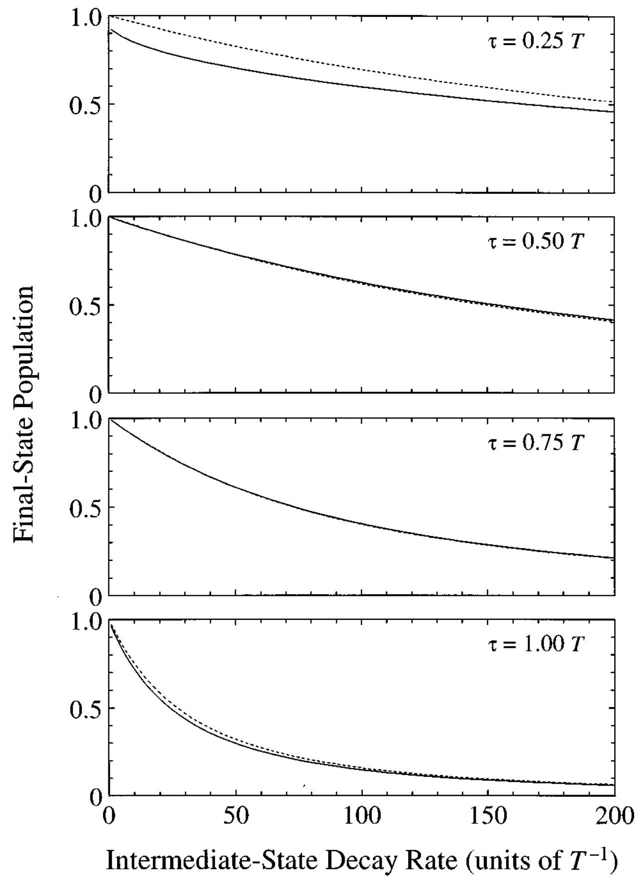

FIG. 6. The final-state population as a function of the intermediate-state decay rate for Gaussian pulses (27) in the *counterintuitive* order with $\alpha=20$ and $\delta=0$ for several pulse delays τ. The full curves show the exact results, obtained by numerical integration of Eqs. (1), while the dashed curves derive from our analytic approximation (31).

$$P_3^{ci} \sim \exp\left[-\frac{4(\tau/T)^2+\pi/4}{3(\tau/T)} e^{2(\tau/T)^2} \frac{\gamma}{\alpha^2} + O(|A|^{-3})\right], \quad (|A|\gg 1). \quad (32)$$

From here we find that

$$c(\tau/T) \approx \frac{3(\tau/T)\ln 2}{4(\tau/T)^2+\pi/4} e^{-2(\tau/T)^2}. \quad (33)$$

Insofar as the detuning δ does not appear in the leading term of Eq. (32), the coefficient $c(\tau/T)$ does not depend on it in the lowest order. This is consistent with our conclusions in Sec. II D 2 that P_3^{ci} depends on δ very weakly for large α; we have also checked this numerically. Formula (33) suggests that $c(\tau/T)$ rises from zero at $\tau=0$ to its maximum value of about 0.455 at $\tau\approx 0.302$ T and then decreases in a near-Gaussian fashion with τ. In Fig. 7, Eq. (33) is compared to the exact numerical values (calculated for $\delta=0$). The agreement observed in the overall behavior of $c(\tau/T)$, the maximum position, and the maximum value, is very good, particularly in view of the fact that Eq. (33) has been derived by using several successive approximations: replacing Eqs. (1) with Eqs. (7) by adiabatic elimination of the intermediate state $|2\rangle$; matching the Gaussian model (27) to the analytic

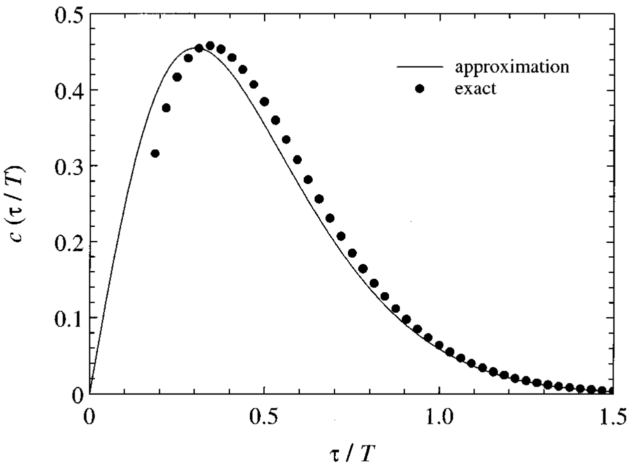

FIG. 7. The coefficient $c(\tau/T)$ in Eq. (10) plotted as a function of the pulse delay for Gaussian pulses (27) in the counterintuitive order. The dots show the exact numerical values, while the solid curve is our analytic approximation (33).

model (28); replacing the γ functions in Eq. (31) by their Stirling asymptotics. The decrease of $c(\tau/T)$ at small τ/T is because of the larger pulse area needed to avoid the population loss, which gets stronger when the pulses overlap too much. The decrease of $c(\tau/T)$ at large τ/T is due to the larger pulse area needed to ensure sufficient adiabaticity.

V. CONCLUSIONS

We have examined the effect of the irreversible dissipation from the intermediate state $|2\rangle$ on the efficiency of population transfer by delayed pulses in three-state systems. We have shown that this effect is much more pronounced for the intuitive pulse sequence because then the intermediate state is significantly populated during the transfer. For intuitive pulses, the transfer efficiency decreases exponentially with the decay rate Γ, the dominant loss mechanism being the direct dissipation from state $|2\rangle$. For the counterintuitive pulse sequence, the losses occur by two mechanisms. The first, which dominates at small and medium decay rates, is the dissipation of the population which visits state $|2\rangle$ due to imperfect adiabaticity. The second is the quantum overdamping, which dominates for large Γ and shows up as effective decoupling of the three-state system from the external fields. These two mechanisms lead to different damping of the transfer efficiency with Γ: exponential at small Γ and polynomial at large Γ. Several general approximations to the final-state population have been derived. Moreover, the range of decay rates, over which the transfer efficiency remains high, has been found to be proportional to the squared pulse area. We have checked our general conclusions with an analytically solvable model in Sec. III and for Gaussian pulses in Sec. IV. In the case of Gaussians, we have derived analytic approximations for the final-state population and for the width of the region of high transfer efficiency.

[1] U. Gaubatz, P. Rudecki, M. Becker, S. Schiemann, M. Külz, and K. Bergmann, Chem. Phys. Lett. **149**, 463 (1988); J. R. Kuklinski, U. Gaubatz, F. T. Hioe, and K. Bergmann, Phys. Rev. A **40**, 6741 (1989); U. Gaubatz, P. Rudecki, S. Schiemann, and K. Bergmann, J. Chem. Phys. **92**, 5363 (1990); B. W. Shore, Contemp. Phys. **36**, 15 (1995); N. V. Vitanov and S. Stenholm, Opt. Commun. **127**, 215 (1996).

[2] N. V. Vitanov and S. Stenholm, Phys. Rev. A **55**, 648 (1997).

[3] N. V. Vitanov and S. Stenholm, Opt. Commun. **135**, 394 (1997).

[4] C. E. Carroll and F. T. Hioe, Phys. Rev. Lett. **68**, 3523 (1992); Phys. Rev. A **47**, 571 (1993); Phys. Lett. A **199**, 145 (1995); Phys. Rev. A **54**, 5147 (1996); L. P. Yatsenko, R. G. Unanyan, K. Bergmann, T. Halfmann, and B. W. Shore, Opt. Commun. **135**, 406 (1997).

[5] T. Nakajima, M. Elk, J. Zhang, and P. Lambropoulos, Phys. Rev. A **50**, R913 (1994).

[6] N. V. Vitanov and S. Stenholm (unpublished).

[7] V. M. Akulin and W. P. Schleich, Phys. Rev. A **46**, 4110 (1992).

[8] N. V. Vitanov and S. Stenholm, Phys. Rev. A **55**, 2982 (1997); the factor $1/(4\pi^2)$ on the right-hand side of Eq. (18) should be $1/(2\pi^2)$.

[9] It is also more difficult to satisfy the adiabaticity condition for the intuitive order, see Ref. [2].

[10] The effective decay rate of the intermediate state can be controlled experimentally for example, by coupling this state to the continuum by a third cw laser.

[11] M. V. Berry, Proc. R. Soc. London, Ser. A **429**, 61 (1990); R. Lim and M. V. Berry, J. Phys. A **24**, 3255 (1991); M. V. Berry and R. Lim, *ibid.* **26**, 4737 (1993).

[12] Some related discussion can also be found in Ref. [5].

[13] L. Allen and C. R. Stroud, Jr., Phys. Rep. **91**, 1 (1982); S. Stenholm, *Foundations of Laser Spectroscopy* (Wiley, New York, 1984).

[14] W. Magnus, Commun. Pure Appl. Math. **7**, 649 (1954); P. Pechukas, J. Chem. Phys. **44**, 3897 (1966); M. M. Maricq, *ibid.* **86**, 5647 (1987).

[15] L. Allen and J. H. Eberly, *Optical Resonance and Two-Level Atoms* (Dover, New York, 1987); F. T. Hioe, Phys. Rev. A **30**, 2100 (1984).

[16] Yu. N. Demkov and M. Kunike, Vestn. Leningr. Univ. Fiz. Khim. **16**, 39 (1969); F. T. Hioe and C. E. Carroll, Phys. Rev. A **32**, 1541 (1985); J. Zakrzewski, *ibid.* **32**, 3748 (1985); K.-A. Suominen and B. M. Garraway, *ibid.* **45**, 374 (1992).

[17] N. Rosen and C. Zener, Phys. Rev. **40**, 502 (1932); N. V. Vitanov, J. Phys. B **27**, 1351 (1994).

[18] *Handbook of Mathematical Functions*, edited by M. Abramowitz and I. A. Stegun (Dover, New York, 1964).